J. Phys.: Condens. Matter **12** (2000) A391–A397. Printed in the UK PII: S0953-8984(00)09387-5

Rotational freezing in plastic crystals: a model system for investigating the dynamics of the glass transition

F J Bermejo†, M Jiménez-Ruiz†, A Criado†, G J Cuello†, C Cabrillo†, F R Trouw‡, R Fernández-Perea‡, H Löwen§ and H E Fischer‖

† Consejo Superior de Investigaciones Científicas, Serrano 121-123, E-28006 Madrid, and Departamento de Física de la Materia Condensada, Universidad de Sevilla, PO Box 1065, E-41080 Seville, Spain

‡ Argonne National Laboratory, Argonne, IL 60439, USA

§ Institut für Theoretische Physik II, Heinrich-Heine-Universität, Universitätsstrasse 1, D-40225 Düsseldorf, Germany

‖ Institut Laue–Langevin, BP 156X, F-38042 Grenoble Cédex 9, France

Received 29 September 1999

Abstract. The dynamics of the rotational freezing transition of the rotator phase (RP) crystal of ethanol into its orientational glass (OG) phase is monitored by measurements of molecular rotational components in the quasielastic neutron scattering spectrum. Such a transition is known to share several features in common with the canonical liquid $\longrightarrow$ glass transition (both taking place within the same temperature interval), and therefore some of the results from such a study should be of relevance for our understanding of the latter. We show that the basic features of the RP $\longrightarrow$ OG transition can be understood in terms of a hard-needle model by means of a mapping of the aspect ratio onto a temperature scale.

Freezing of rotational motions in some plastic (rotationally disordered or rotator phase) crystals is known to take place by means of a sluggish transformation leading to an orientationally disordered crystal state (orientational glass, OG) where molecular rotations are completely arrested [1]. Such transitions are signalled by jumps in the specific heat as well as in the coefficient of thermal expansion without involving any further structural change (the same crystal lattice is retained upon freezing). That is, they share the basic fingerprints of the non-equilibrium transition which occurs by rapid cooling of a liquid leading to an amorphous solid, and therefore are regarded as true 'glass transitions'.

The liquid $\longrightarrow$ glass transition may either be viewed as a purely dynamical phenomenon without any associated changes in static quantities [2] or understood as a remnant of an underlying thermodynamic phase change [3, 4] which is partially hidden for purely kinetic reasons. Arguments in favour of both points of view are partially supported by experimental data, and both alternatives are grounded on fairly well elaborated theoretical frameworks such as kinetic theories of the mode-coupling family [2] or the treatments concerning the dynamics of critical phenomena [3].

The main difficulties in evaluating the merits of the two approaches concern the wide range of complex phenomena involved within the glass transition of a real material which hide some of the behaviours expected to appear as characteristic signatures of the transition. In fact, most systems where detailed studies can be carried out within the deeply supercooled

0953-8984/00/SA0391+07$30.00

liquid do show a rich variety of phenomena such as molecular rotations and/or low-energy vibrations, which are strongly coupled to the translational dynamics due to the huge viscosity characteristic of temperatures near the glass transition point T_g.

In contrast, the glass transition leading from rotator phase crystals (RP) to the orientationally disordered (orientational glass, OG) state can possibly be understood as a purely dynamic crossover. To assess such characteristics we compare neutron scattering data for ethanol across the above-mentioned transition with those resulting from a simple, albeit non-trivial, model [5] which exhibits a purely dynamical crossover. We find very similar signatures of the RP $\longrightarrow$ OG transition in the two cases, which lends strong support to the view that such a transition is a purely dynamic phenomenon.

Our choosing of this particular sample follows previous work [7, 8] which shows that it presents some important advantages over other systems studied so far [6]. In particular, ethyl alcohol has the unique feature that it can be prepared in two different phases showing glassy behaviour at the same temperature, one of these phases having structural disorder (liquid and glass) and the other having orientational disorder (RP and OG). In the disordered crystals the molecular centres of mass sit at the nodes of a body-centred-cubic (bcc) lattice [9, 10], and melting into the RP is signalled by a jump in specific heat [8], which amounts to about 80% of that of the liquid $\longrightarrow$ glass one, as well as a jump in the thermal expansivity. Both liquid $\longrightarrow$ glass and the RP $\longrightarrow$ OG transitions occur in a temperature interval centred at about 97 K. Such proximity of the two transitions was also revealed by dielectric spectroscopy [11] where both α- and sub-T_g relaxations appear that are astoundingly close in frequency and temperature dependence. Hence the canonical glass transition seems to be dominated by the freezing of the orientational degrees of freedom. If there is evidence that the RP $\longrightarrow$ OG transition is purely dynamical, the same conclusion should apply for the canonical glass transition. Hence our study even sheds new light on the nature of the structural liquid–glass transition.

Neutron quasielastic scattering experiments were carried out to explore the microscopic dynamics within scales of about 1 meV ($\approx$1.5 ps^{-1}) and of about 1 μeV, using the QENS spectrometer at the IPNS (Intense Pulsed Neutron Source), as well as the IN16 backscattering spectrometer at the Institut Laue–Langevin (Grenoble). Partially (C_2D_5OH) deuterated samples were employed to monitor its state (glass, liquid or cubic crystal) by means of inspection of the diffraction patterns.

The measured spectra show at both at meV and μeV scales a strong elastic (resolution-limited) component plus a quasielastic contribution as shown in figure 1. The temperature dependence of the quasielastic linewidths is shown in figure 2. Apart from details arising from the rather different frequency windows of the two spectrometers, the same dependence is observed, showing that the broadening of the quasielastic spectrum increases in a non-trivial fashion through the rotational melting transition.

The assignment of the observed broadenings to underlying microscopic motions requires the use of a model to represent the dynamics [12]. From symmetry considerations one expects the molecular motions to be describable in terms of formalisms such as that developed to account for the neutron scattering law for reorientations about [100], [110] and [111] axes of a cubic lattice [13]. It predicts a scattering law given in terms of four classes of molecular rotations with jump rates τ_j^{-1}, $j = 1$–4. Two of those are set from the (inverse of the) linewidth of the quasielastic spectra measured at both instruments. However, their assignment to specific motions requires additional information from some other sources. To this end, we have carried out molecular dynamics simulations on the NPT-ensemble (the cell shape is allowed to fluctuate) using a realistic model potential for the microscopic interactions [14]. The results of this endeavour were gratifying since: (a) the equilibrium lattice structure is

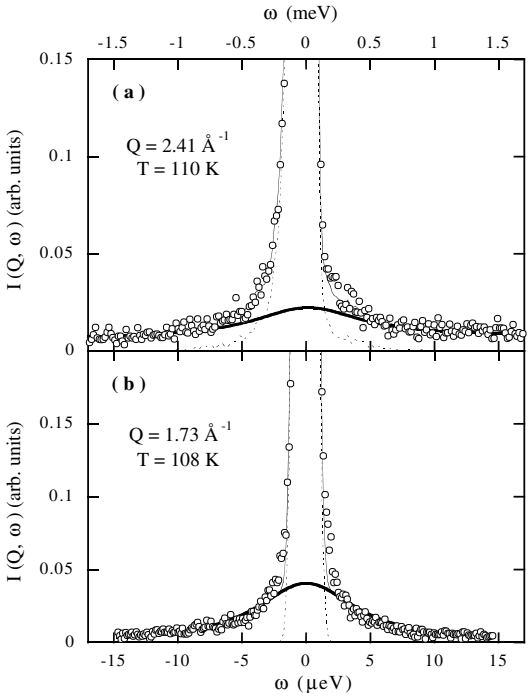

Figure 1. Spectra as measured on both QENS and IN16 spectrometers. Model fits are shown by thin solid lines. Dashed and thick solid lines correspond to the elastic and quasielastic components respectively.

reproduced; (b) freezing of rotational motions occurs below 100 K; and (c) the crystal structure becomes unstable above 120 K, which is quite close to the experimental value. From analysis of the computed trajectories, it was found that molecules will reorient between some 24 preferred orientations with vastly different rates. Reorientations leaving unaffected the most preferred orientations (a C–O bond along the [001] direction and a C–C bond close to $[11\bar{1}]$, and those related by symmetry) were found to take place on the picosecond scale, whereas far more infrequent jumps occurring on scales of hundreds of picoseconds were also monitored. The calculated intermediate dynamic structure factor $F_{MD}(Q, t)$ showed strong deviations from single-exponential behaviour and, as expected, four different decays were needed to fully account for its shape. Two of the fitted decays were found to be within the frequency windows covered by the experiments and therefore we identify the relaxations observed on both instruments with two different motions of the kinds referred to above.

Apart from the variation with temperature of the linewidth, the RP $\longrightarrow$ OG transition is also followed by a rise with temperature of the quasielastic intensity and the concomitant decrease of the elastic peak, as shown in figure 3. As seen there, the transition is very nicely monitored by following the transfer of spectral intensity from elastic to quasielastic (or inelastic) scattering and this shows very similar characteristics for the two frequency windows.

From the data given above it is seen that molecular rotations occur in the rotator phase crystal on picosecond and nanosecond scales at temperatures where the main α-relaxation explored by dielectric spectroscopy [11] already reaches macroscopic relaxation times. Well below 85 K, rotational freezing seems complete, and all the molecular degrees of freedom which are thermally excited will contribute to the spectrum as inelastic (i.e. finite-frequency)

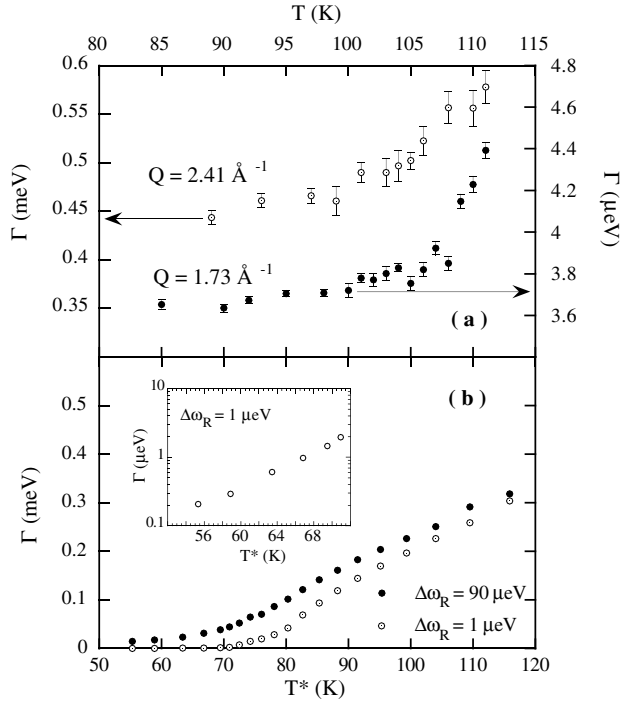

Figure 2. (a) The temperature dependence of the quasielastic linewidth as measured on the QENS (filled) and IN16 (open symbols) spectrometers. (b) The variation of the width of $\Phi(\omega)$ as calculated from results for systems of hard needles. The inset shows data on the μeV scale in a semi-logarithmic plot.

signals [8]. This is in very good agreement with specific heat data [8], which also shows that the extent in temperature of the transition is quite comparable to that evidenced by the present data (i.e. about 18 K).

Some conceptually simple models have been reported in the literature which exhibit a purely dynamical glass transition. Among these, that developed by Renner *et al* [5] consisting of a set of hard infinitely thin needles on a lattice seems most appealing. Such bodies are executing free rotations between elastic collisions having their centres of mass located at the nodes of a cubic lattice. The only control parameter is the ratio $\ell = L/a$ of the needle length L to the lattice constant a [15]. Since the excluded volume of the needles is zero, all the static properties of the model are trivial (i.e. there are no static correlations). However, its transport and dynamic properties exhibit a strong dependence on ℓ. The dynamics of such a model was investigated by computer simulations carried out on a system of $N = 432$ infinitely thin needles with a homogeneous line mass density m/L whose centre-of-mass coordinates are fixed onto a bcc lattice in a periodically repeated cubic simulation box. From the calculated trajectories we obtained the time-autocorrelation function for the needle orientations as

$$\Phi_1(t) = \left\langle \frac{1}{N} \sum_{i=1}^{N} \vec{u}_i(0) \cdot \vec{u}_i(t) \right\rangle \tag{1}$$

where the angular brackets denote the canonical average and $\vec{u}_i(t)$ is the time-dependent trajectory of the unit vector describing the orientation of the ith needle. We explored the range $1.0 \leqslant \ell \leqslant 5.0$. The system was left to evolve over a long time corresponding to 10^6 collisions.

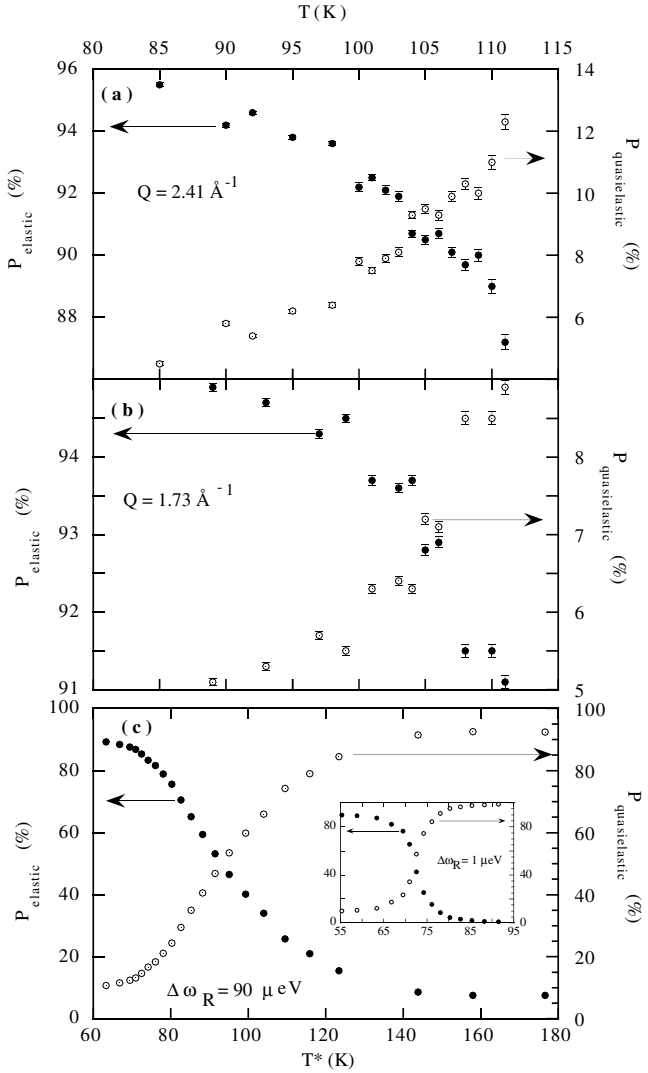

Figure 3. (a) The temperature dependence of the elastic (solid) and quasielastic (open symbols) intensities across the RP $\longrightarrow$ OG transition measured on the QENS spectrometer. (b) The same data measured on IN16. (c) Contributions from the $\Phi(\omega)$ to the elastic (solid) and quasielastic (open symbols) frequency windows versus the equivalent temperature T^* for the resolution width $\Delta\omega_R = 90$ μeV. The inset shows data for the resolution width $\Delta\omega_R = 1$ μeV.

As a result, as ℓ increases, the relaxation of $\Phi_1(t)$ becomes more and more sluggish, and for $\ell \sim 3.4$ the autocorrelation is almost blocked on the timescale explored in the simulation. For $\ell = 4.5$ the orientational autocorrelation is almost equal to unity—that is, orientations become frozen within a very narrow solid angle. Let us now discuss how to establish a link between the needle model and our experimental data. First, as already mentioned, we choose a bcc lattice with a lattice constant of $a = 5.36$ Å to mimic the real RP crystal. Second, the timescale can be mapped directly. In the needle model it is set by the time $\tau \equiv \sqrt{mL^2/24k_BT}$. If we identify the moment of inertia of the needles $J = mL^2/12$ with that of one ethanol molecule ($J = 0.741 \times 10^{-45}$ kg m^2), we obtain that the timescale τ corresponds to $\approx$1 ps at

$T = 100$ K which clearly sets the short-time rotational dynamics of ethanol. Consequently we can translate experimental frequencies into simulation data and vice versa. Finally, in the athermal needle model, only ℓ enters, whereas temperature is the crucial parameter for our measurements. In order to establish a mapping between ℓ and T, we write an inverse effective ratio $1/\ell$ as a Boltzmann factor $1/\ell = A\exp(-E/k_BT)$ [16]. Clearly the limit $\ell \to \infty$ corresponds to zero temperature. The two free constants, namely the amplitude A and the energy scale E, are determined as follows.

(a) First we recall that if the needle length is smaller than the nearest-neighbour distance $\sqrt{3}a/2$ the needles are non-interacting free rotators which corresponds to infinite temperature and this serves to set the amplitude $A = 2/\sqrt{3} = 1/\ell_0$.
(b) Second, the energy scale E should correspond to the experimental glass transition temperature such that $E = k_BT_g$.

Hence, the translation of temperatures in the experiment into the effective ratios ℓ of our model is given by $\ell = \ell_0 \exp(T_g/T^*)$.

Because both experiment and computer simulations on the needle model or using a full microscopic potential share the same lattice structure, one expects that the shape of the $\Phi_1(t)$ autocorrelations will resemble that of $F_{MD}(Q,t)$ referred to above; this is a substantial departure from exponential behaviour arising from motions involving well separated timescales. That this is indeed the case is demonstrated by data shown in reference [5]. Also, our calculated functions did require a minimum of three exponentials to account for their shape.

A comparison between experimental and model results is enabled by calculation of a quantity equivalent to the measured spectrum such as the Fourier transform of $\Phi_1(t)$. We have numerically transformed our computer simulation data on $\Phi_1(t)$ into the frequency domain and convoluted them with the resolution function characteristic of each spectrometer. The resulting functions $\Phi(\omega)$ were split into elastic and quasielastic parts depending upon the width $\Delta\omega_R$. The linewidth and the amplitude of the quasielastic parts were determined as was done for the experimental data. The results for the widths corresponding to both resolution functions are given in figure 2, and those for the intensity ratios in figure 3. Note that the simulated data were always expressed as temperatures via the translation given above. One clearly sees a kink in the Lorentzian intensities as well as in the linewidths of both experiments at meV and μeV scales and in the needle model data at temperatures of 95 K and 75 K respectively. Such features appear at the same temperatures irrespective of the scale of frequencies being explored. In other words, all rotations slow down with decreasing temperature showing fairly similar dependences on temperature of their characteristic jump rates. This is a clear-cut fingerprint of the orientational glass transition. On the other hand, the elastic intensities also exhibit similar kinks. The only difference between experiment and the model is in the relative magnitudes of the changes in elastic and quasielastic intensities as well as in the absolute values of the linewidths. The experiment contains a strong scattering component seen as an elastic peak (unresolved) with an intensity modulated by a strong Debye–Waller factor which includes contributions from both centre-of-mass motions and librational excursions. Such a contribution is obviously absent in the model which, by construction, shows no strictly elastic component. The relative widths of the crossovers are about 25 K in experiment and $\approx$70 K for the needle model, a difference expected from the absence in the latter case of a true interaction potential.

In conclusion, we have shown that the essential features of the scattering data across the orientational glass transition can be understood in terms of a purely dynamical model. The fingerprints of the transition as revealed by cusps in the inelastic scattering are very similar in the experiment and in the model. The implications of such an analogy in dynamic behaviour

can, in the light of previous data, extend to a large extent to the canonical glass/liquid transition, inasmuch as the latter must carry a large rotational component (in fact, the jump in specific heat at the glass and OG $\longrightarrow$ RP transitions corresponds to an activation of $\approx$2.8 degrees of freedom in the latter and about 3.7 in the former, the extra degree surely assignable to translational motions).

Acknowledgments

This work was supported in part by the US Department of Energy, Basic Energy Sciences—Materials Sciences, under Contract W-31-109-ENG-38 and DGICYT (Spain) Grant No PB95-0075-C03-01.

References

[1] Loidl A and Böhmer R 1994 *Disorder Effects on Relaxational Processes* ed R Richert *et al* (Heidelberg: Springer) p 659
[2] Götze W 1991 *Liquids, Freezing and Glass Transition* ed J-P Hansen *et al* (Amsterdam: North-Holland)
[3] Sethna J P *et al* 1991 *Phys. Rev.* B **44** 4943
[4] Bletry J 1996 *Z. Naturf.* a **51** 87
[5] Renner C *et al* 1995 *Phys. Rev.* E **52** 5091
[6] Descamps M *et al* 1994 *Quasielastic Neutron Scattering* ed J Colmenero *et al* (Singapore: World Scientific) p 107
[7] Ramos M A *et al* 1997 *Phys. Rev. Lett.* **78** 82
[8] Talón C *et al* 1998 *Phys. Rev.* B **58** 745
[9] Bermejo F J *et al* 1997 *Phys. Rev.* B **56** 11 536
[10] Fayos R *et al* 1996 *Phys. Rev. Lett.* **77** 3823
[11] Miller M *et al* 1998 *Phys. Rev.* B **57** R13 977
Jiménez-Ruiz M *et al* 1999 *Phys. Rev.* B **59** 9155
[12] Lovesey S W 1984 *Theory on Neutron Scattering from Condensed Matter* (New York: Oxford Science) p 326
[13] Bée M 1988 *Quasielastic Neutron Scattering* (Bristol: Hilger)
[14] Criado A *et al* 1999 *Proc. 6th Workshop on Disorder in Molecular Solids (Garchy, France, 1999); Phys. Rev.* B submitted
[15] Frenkel D and Maguire J F 1981 *Phys. Rev. Lett.* **47** 1025
Frenkel D and Maguire J F 1983 *Mol. Phys.* **49** 503
[16] A more elaborate mapping is known for hard spheres where the effective diameter is also taken as an averaged Boltzmann factor in order to match the second virial coefficient; see e.g.
Barker J A *et al* 1976 *Rev. Mod. Phys.* **48** 587